THE EFFECT OF LAI BASED MODIS VEGETATION INDEX IN DIFFERENT SCALE TO ESTIMATE GROSS PRIMARY PRODUCTIVITY

Supannika Potithep, Postdoctoral Researcher
Rikie Suzuki, Team Leader
Research Institute for Global Change
Japan Agency for Marine-Earth Science and Technology
3173-25 Showa-machi, Kanazawa-ku
Kanagawa 236-0001 Japan
spotithep@jamstec.go.jp
rikie@jamstec.go.jp

ABSTRACT

The Moderate Resolution Imaging Spectroradiometer (MODIS) is the primary NASA Earth Observing System instrument monitoring the seasonality of global terrestrial vegetation. MODIS products, such as the MODIS Vegetation Index (VI), Normalized Difference Vegetation Index (NDVI) and Enhanced Vegetation Index (EVI), are commonly used in ecological modeling. The difference spatial resolutions (250, 500, 1000 and 5600 m) may cause the error in the output. In this study, the 3-PGS (Physiological Principles Predicting Growth using Satellite data) model was used to examined the errors of gross primary productivity (GPP) based difference spatial resolutions. First, *in situ* Leaf Area Index (LAI) was compared with NDVI and EVI from Hemispherical Spectroradiometer (HSSR) to find the relationship. Then, these relationships were applied to the model for estimating GPP as the final output. From the results, GPP based on MODIS NDVI at spatial resolution 250 m was performed the less error around 9.12%, whereas GPP based MODIS on EVI at spatial resolution 1000 m was performed the less error around 5.76%. GPP based on MODIS NDVI and EVI at spatial resolution 5600 m were showed the biggest error with 18.47% and 13.02%, respectively. However, the global spatial resolution can be accepted for applying to the model, based on one point, with the error around 20%.

INTRODUCTION

The Moderate Resolution Imaging Spectroradiometer (MODIS) satellite imager has a standard suite of global products characterizing vegetation cover, LAI, VI (NDVI and EVI), GPP, and net primary productivity (NPP) at multi scale (Justice et al., 2002; Running et al., 2004). Several studies have compared information from MODIS products to data from a global ground-based monitoring network of micro-meteorological tower sites (FLUXNET; Baldocchi et al., 2001) and regional networks such as AmeriFLUX (Law et al., 2002) and AsiaFlux (Yamamoto, 2002), where continuous measurements of meteorological data and eddy covariance flux provide GPP estimates (Saigusa et al., 2002; Nakai et al., 2003; Heinsch et al., 2006). Although this validation is needed to improve the performance of MODIS products, it is challenging to perform because of the difficulty of direct measurement at the appropriate scale (Cohen et al., 2003; Gebremichael & Barros, 2006).

The different spatial resolution is one of main causes that affected to the result from the model. Global spatial resolution provides the wide information in regional and global view. When it was zoomed in to the local view, it showed the uncertainty value. Even though the high spatial resolution can perform more accuracy than the low spatial resolution, it still contains some error. Recently, several researchers used the high spatial resolution to apply to the ecological model and then scaling up to the regional and global scale for extrapolated the data. However, there is some problem regarding the scaling up method.

In this study, we examined the effect of different spatial resolution to GPP estimation based MODIS Vegetation Index (VI) by the 3-PGS (Physiological Principles Predicting Growth using Satellite data) model. The potential of global spatial resolution was investigated to apply in the local ecological model. All of the results from the different spatial resolution were compared to estimated GPP from a flux tower at the study site for accuracy assessment.

3-PGS MODEL

The 3-PGS model (Coops et al., 1998) is a developed version of 3-PG, which was intended to bridge the gap between growth and yield and carbon balance models (Landsberg & Waring, 1997). 3-PG requires weather and site data. The needed meteorological data include mean temperature (°C), mean solar radiation (MJ m^{-2} day^{-1}), total precipitation (mm), frost days (days per month), and vapor pressure deficit (mbar). Site factor parameters are latitude, maximum available soil water (mm), soil texture, and fertility rating. In 3-PGS, satellite imagery provides additional data that drive the model in estimating LAI, generating an important model parameter to determine radiation intercepted by the canopy (absorbed photosynthetically active radiation [APAR]). Other required input data are the same as those in the original 3-PG model. GPP is calculated by converting APAR to GPP using canopy quantum efficiency, which is constrained by environmental conditions (Waring et al., 1998; Sands and Landsberg, 2002; Landsberg et al., 2003). The use of satellite imagery ensures the use of up-to-date ground conditions in the estimation of LAI and evaluation of spatial variability (for more details, see Coops et al., 1998).

3-PGS is applicable to forest plantations and even-aged, relatively homogeneous forests. However, parameterization is needed for different species or vegetation types (Coops et al., 2001a; Coops & Waring, 2001b). The main outputs of the model, which can run monthly or annual time steps for long-term scenarios, are GPP, NPP, and biomass. In this study, we excluded NPP and biomass and focused on GPP estimation. 3-PGS estimates LAI from the NDVI values of each pixel. In this study, we also examined another vegetation index, EVI, which has been used to estimate LAI and other canopy properties.

METERIALS AND METHODS

Study Site

The study site was located in a deciduous broadleaf forest, the major type of vegetation in Japan, in Takayama, central Japan (36°8′46″N, 137°25′23″E; 1,420 m altitude), at a site where meteorological and ecological parameters have been observed continuously at a flux tower since 1993 (Saigusa et al., 2002). Meteorological data, including air temperature, precipitation, global solar radiation, humidity, wind speed, and soil temperature, are collected every 30 min. During 2004–2006, the mean annual air temperature and annual precipitation were 6.67°C and 2199 mm, respectively. The annual mean solar radiation was 4560 MJ m^{-2}. Snow cover during the winter (December–April) was approximately 1 m in depth. The forest canopy was dominated by *Quercus crispula* and *Betula ermanii*, with heights of 18–20 m. The forest floor was covered by evergreen dwarf bamboo, *Sasa senanensis* (Ito et al., 2005; Ohtsuka et al., 2005). The data used in this study were from 2005–2006.

LAI

LAI data were obtained by using phenology shoot approach and litter trap approach (Nasahara et al., 2008). We carried out leaf seasonality observation by mean of *in situ* observation of sample shoots. We selected 20 shoots samples based on ease of access and the goal of measuring shoots at a variety of positions. The number of leaves on the shoot and the size (length and width) of selected leaves were observed during leaf-expansion season. By approximating the shape of the leaves and assuming that the measured length and width represented the longest and shortest axes of the ellipse, the area of each leaf was estimated. Sum of these leaf areas gave us as estimate of total leaf area on the shoot at that point in time. Then, we obtained a time series for the seasonal changes in total leaf area on each shoot. During leaf-fall season, the litter trap approach was applied. Fourteen litter traps were installed within a 1-ha permanent sample plot. Each trap has an area of 1 m^2. The litter caught in the traps were recovered during leaf-fall season. The leaves were dried at approximately 70°C more than 48 hours. Then, we measured the dry mass of leaves. LAI were calculated by dividing this mass by the average leaf area. By combining two approaches, we extrapolated the results to cover throughout the leaf-expansion/fall season.

Ground Observations

To investigate the relationship between LAI and VI, we installed a hemispherical spectroradiometer (HSSR) system to monitor spectral features of vegetation conditions at fine-temporal and fine-spectral resolutions. The spectral range was 300–1100 nm, with a 3.3-nm spectral interval and 10-nm half-band width (MS-700, Eko Instruments Co. Ltd.). The computer-controlled rotating stage (Hayasaka Rikoh Co.) could be directed upward and downward of the spectroradiometer every 10 min (Nishida, 2007). Spectral data measured with this instrumentation avoid cloud contamination and atmospheric noise effects. Using HSSR spectral reflectance data, we calculated NDVI and EVI, using the 620–670-nm spectral range for the red band (*RED*), 841–876 nm for the near-infrared band (*NIR*), and 459–479 nm for the blue band (*BLUE*). These spectral bands correspond to MODIS bands 1, 2 and 3, respectively. NDVI (Rouse et al., 1973) and EVI (Huete et al., 2002) are common VIs used to calculate LAI from the following equations:

$$\text{NDVI} = (NIR - RED)/(NIR + RED) \quad (1)$$

$$\text{EVI} = G[(NIR - RED)/(NIR + C_1(RED) - C_2(BLUE) + L)] \quad (2)$$

where C_1 and C_2 are coefficients of aerosol resistance and L is a canopy background adjustment. Normally, the values of G, L, C_1, and C_2 are 2.5, 1, 6, and 7.5, respectively. The range varies from –1 (bare soil) to 1 (healthy vegetation). NDVI and EVI values calculated from HSSR were referred to as $NDVI_{HSSR}$ and EVI_{HSSR}. LAI data collected by fish eye algorithm on the same date were then compared to $NDVI_{HSSR}$ and EVI_{HSSR}.

In addition, daily GPP data were analyzed from flux measurements, based on the eddy-covariance method, which is the sum of the negative net ecosystem exchange observed via eddy-covariance measurements and ecosystem respiration computed by extrapolating the nighttime flux of net ecosystem productivity (Saigusa et al., 2002; Saigusa et al., 2005). The gap-filling method was used to fill in missing data and remove GPP values less than zero.

Remote Sensing Images Analysis

We used MODIS images in this study because of their significant temporal and areal coverage. A key instrument of the NASA Earth Observation System satellite, which monitors the global environment, MODIS provides a wide range of wavelengths from 0.4 to 14.4 nm, visible to thermal infrared, in 36 spectral bands. The spatial resolution is 250, 500, and 1000 m. To avoid the effects of cloud contamination and atmospheric aerosols, we selected composite images to increase the quality of spectral reflectance (Holben, 1986; van Leeuwen et al., 1999; Duchemin et al., 2002).

In this study, the different of spatial resolutions were examined how it affects to GPP estimation by 3-PGS. For NDVI and EVI data, we used MODIS/Terra Vegetation Indices 16-day L3 Global. The available spatial resolutions were 250, 500, 1000 and 5600 m. Both VIs were used to evaluate LAI data based on the LAI–VI_{HSSR} relationship.

All MODIS products were downloaded from the NASA Land Processes Distributed Active Archive Center using the NASA Warehouse Inventory Search Tool (https://wist.echo.nasa.gov/api/). The data were collected in 2005–2006. We extracted the single pixel corresponding to the study site from the satellite image. The footprint of study area was approximately 1 km^2.

RESULTS AND DISCUSSIONS

LAI-VI_{HSSR} Relationship

The LAI–$NDVI_{HSSR}$ and LAI–EVI_{HSSR} relationships were examined to assign the appropriate VI_{HSSR} for LAI estimation. Figure 1 shows the linear relationship between LAI and both $NDVI_{HSSR}$ and EVI_{HSSR}. With $r^2 = 0.91$,

$NDVI_{HSSR}$ showed a higher significant relationship to LAI than did EVI_{HSSR} ($r^2 = 0.88$). However, both LAI–$NDVI_{HSSR}$ and LAI–EVI_{HSSR} relationship was not exactly linear, as its values were saturated when the LAI value was high and the effect of background reflectance at the beginning of growing season.

The equations obtained from both LAI–$NDVI_{HSSR}$ and LAI–EVI_{HSSR} relationships were applied to 3-PGS for estimating the LAI value from MODIS NDVI and EVI.

GPP Estimation Based Various Spatial Resolutions

The seasonal pattern of *in situ* GPP showed the typical phenological pattern of a deciduous broadleaf forest. *In situ* GPP values were near zero in winter from November to April, as the deciduous-dominated canopy was bare. GPP began to increase from the onset of leaf-out in late April and reached its saturation stage peak from the end of May to September. Leaf senescence (leaf coloring) began in October, and GPP began decreasing to zero. Hence, GPP values in winter were ignored for validation. To compare GPP based on satellite imagery to *in situ* GPP in 2005 to 2006, we recalculated *in situ* GPP as an average 16-day value for GPP based on MODIS NDVI and MODIS EVI.

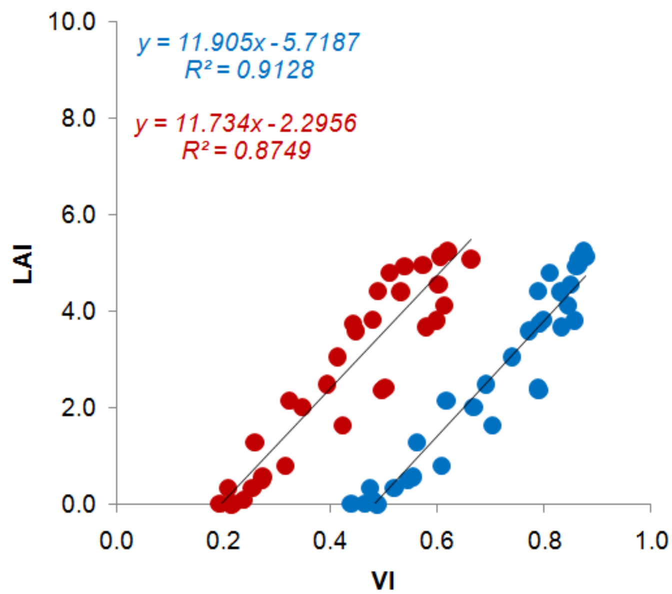

Figure 1. The relationship between LAI and $NDVI_{HSSR}$ (blue circle) and LAI and EVI_{HSSR} (red circle) at Takayama.

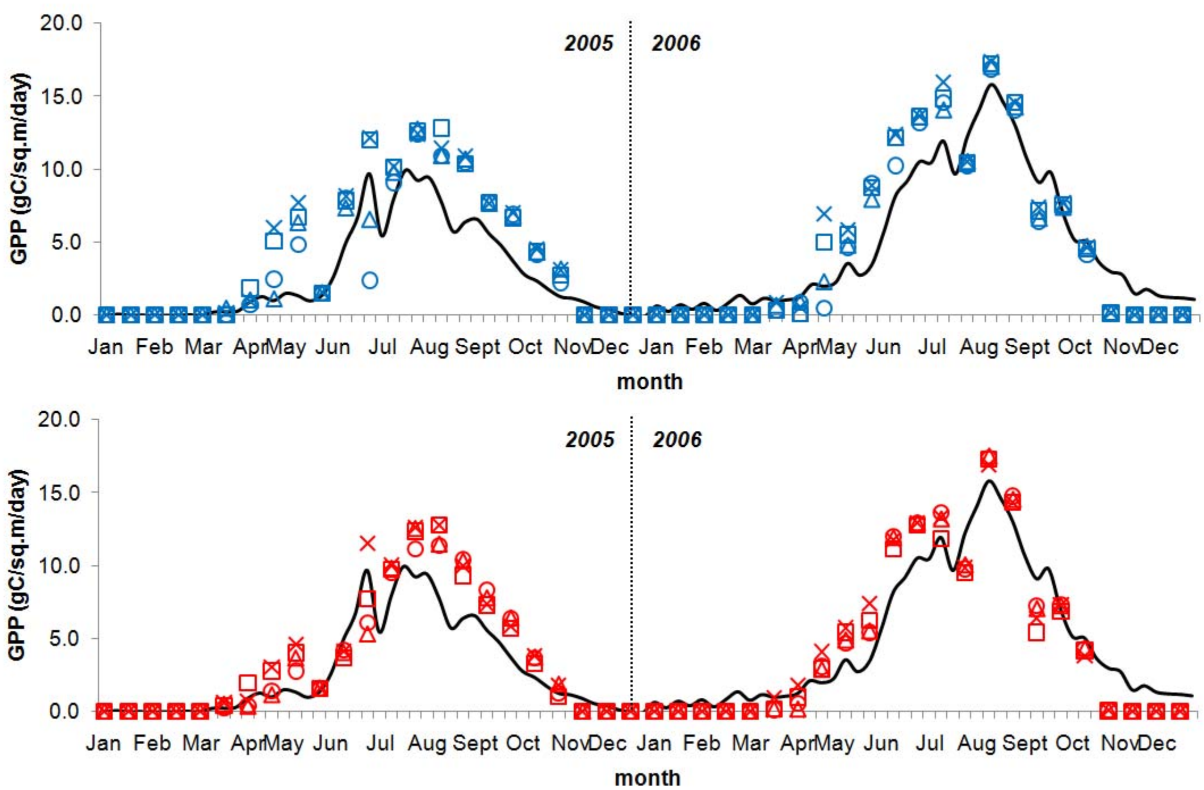

Figure 2. The seasonal pattern of GPP based MODIS NDVI (blue signs) and MODIS EVI (red signs) in different spatial resolutions from 250 (circle), 500 (triangle), 1000 (rectangular) and 5600 (cross) m.

Figure 2 presents the seasonal pattern of GPP estimation against *in situ* GPP. All spatial resolutions provided the overestimated GPP. GPP based on MODIS NDVI at spatial resolution 500 m showed the best agreement to *in situ* GPP (r^2 = 0.78), whereas GPP based on MODIS EVI at spatial resolution 250 m showed the best agreement to *in situ* GPP (r^2 = 0.72). GPP based on MODIS NDVI and EVI at spatial resolution 5600 m presented the lowest of r^2 values as 0.62 and 0.68, respectively. In the falling season (late August to October), GPP estimation among spatial resolutions were not much difference, presented the similar values. However, some different was showed in the growing season especially in the beginning of growing season due to the effect of background reflectance. MODIS NDVI accounted the value of forest floor so than it provided larger overestimated GPP values than MODIS EVI.

Errors of GPP Estimations from Different Spatial Resolutions

Comparing of GPP estimations from different spatial resolutions is presented in Figure 3. GPP based on MODIS NDVI at spatial resolution 250 m was performed the less error around 9.12%, whereas GPP based MODIS on EVI at spatial resolution 1000 m was performed the less error around 5.76%. GPP based on MODIS NDVI and EVI at spatial resolution 5600 m were showed the biggest error with 18.47% and 13.02%, respectively. The errors increased as the spatial resolution was coarse in MODIS NDVI. However, the different of spatial resolutions were not affected to the result, the error percentages were presented in similar values around 13-15%.

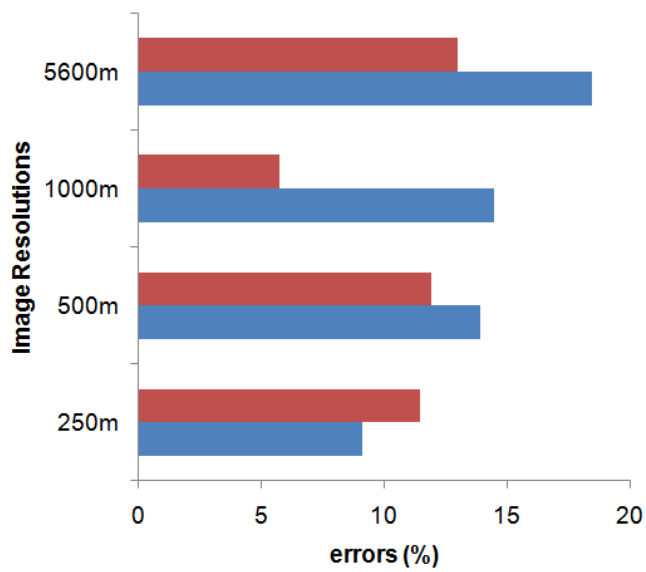

Figure 3. The errors of GPP estimation based MODIS NDVI (blue bar) and MODIS EVI (red bar) in the spatial resolutions from 250 (circle), 500 (triangle), 1000 (rectangular) and 5600 (cross) m.

MODIS NDVI included the forest floor reflectance and saturated when LAI getting bigger, so that the high spatial resolutions can performed better than the low spatial resolution. Since the mixture of objects within the pixel is small. MODIS EVI can reduce the effect of soil reflectance; it is useful for spatial resolution at 1000 m that responds to the flux footprint. The higher spatial resolutions than flux footprint were presented the forest floor than the canopy in the growing season that was affected to the errors. The error results can imply the ecologist and ecological modeler that the global spatial resolution can be accepted for applying to the model, based on one point, with the error around 20%.

CONCLUSIONS

The errors of GPP estimation by difference spatial resolutions were examined for evaluating the effect of result. Before applying MODIS VI to 3-PGS, the relationship between LAI and VI, both NDVI and EVI from HSSR, was investigated. Because of the sensitivity of the LAI–NDVI relationship, we examined another VI (EVI) to assess the potential for generating accurate estimates. The equations for linear regression of LAI-VI_{HSSR} were input to 3-PGS foe LAI estimation based on MODIS VI. The difference spatial resolutions of MODIS VI were used to run the model for checking GPP values. Our comparison of GPP based on MODIS VI with the model results and *in situ* GPP showed that GPP based on MODIS EVI at spatial resolution 1000 m performed the best result, with less error of 5.76%.

ACKNOWLEADGMENTS

The authors would like to give a special thank to National Institute of Advanced Industrial Science and Technology (AIST), and Gifu University for providing the flux tower data at Takayama. Sincerely thanks to Dr.Nishida Kenlo Nasahara and his colleges for kindly supporting LAI data and valuable suggestion on LAI data collection. As well, we appreciated Dr.Shin Nagai for his guidelines at the Takayama site.

REFERENCES

Baldocchi, D., E. Falge, L. Gu, R. Olson, D. Hollinger, and S. Running, 2001. FLUXNET: A new tool to study the temporal and spatial variability of ecosystem-scale carbon dioxide, water vapor and energy flux densities, *Bulletin of the American Meteorological Society*, *82*:2415-2435.

Cohen, W.B., T.K. Maiersperger, Z. Yang, S.T. Gower, D.P. Turner, and W.D. Ritts, 2003. Comparison of land cover and LAI estimates derived from ETM+ and MODIS for four sites in North America: A quality assessment of 2000/2001 provision MODIS products, *Remote Sensing of Environment, 88*:233-255.

Coops, N., R.H Waring., and J.J. Landsberg, 2001a. Estimation of potential forest productivity across the Oregon transect using satellite data and monthly weather records, *International Journal of Remote Sensing*, *22*:3797-3812.

Coops, N.C.,and R.H. Waring, 2001b. The use of multi-scale remote sensing imagery to derive regional estimates of forest growth capacity using 3-PGS, *Remote Sensing of Environment*, *75*:324-334.

Coops, N.C., R.H. Waring, and J.J. Landsberg, 1998. Assessing forest productivity in Australia and New Zealand using a physiologically-based model driven with averaged monthly weather data and satellite derived estimates of canopy photosynthetic capacity, *Forest Ecology and Management*, *104*:113-127.

Duchemin, B., B. Berthelot, G. Dedieu, M. Leroy, and P. Maisongrande, 2002. Normalisation of directional effects in 10-day global syntheses derived from VEGETATION/SPOT: II. Validation of an operational method on actual data sets, *Remote Sensing of Environment, 81*:101-113.

Gebremichael, M., and A.P. Barros, 2006. Evaluation of MODIS Gross Primary Productivity (GPP) in tropical monsoon regions, *Remote Sensing of Environment*, *100*:150-166.

Heinsch, F.A., M. Zhao, S. Running, J.S. Kimball, R.R Nemani, and K.J. Davis, 2006. Evaluation of remote sensing based terrestrial productivity from MODIS using regional Tower Eddy flux network observations, *IEEE TGRS*, *44* :1908-1925.

Holben, B.N.,1986. Characterization of maximum value composites from AVHRR data, *International Journal of Remote Sensing*, *7*:1417-1434.

Huete, A., K. Didan, T. Miura, E.P. Rodriguez, X. Gao, and L.G. Ferreira, 2002. Overview of the radiometric and biophysical performance of the MODIS vegetation indices, *Remote Sensing of Environment*, *83*:195-213

Ito, A., N. Saigusa, S. Murayama, and S. Yamamoto, 2005. Modeling of gross and net carbon dioxide exchange over a cool-temperate deciduous broad-leaved forest in Japan: analysis of seasonal and interannual change, *Agricultural and Forest Meteorology*, *137*:122-134.

Landsberg, J.J., and R.H. Waring, 1997. A generalised model of forest productivity using simplified concepts of radiation-use efficiency, carbon balance and partitioning, *Forest Ecology and Management*, *95*:209-228.

Landsberg, J.J., R.H. Waring, and N.C. Coops, 2003. Performance of the forest productivity model 3-PG applied to a wide range of forest types, *Forest Ecology and Management*, *172*:199-214.

Law, B.E., E. Falge, L. Gu, D. Baldicchi, P. Bakwin, and P. Berbigier, 2002. Environmental controls over carbon dioxide and water vapor exchange of terrestrial vegetation, *Agricultural and Forest Meteorology*, *113*:97-120.

Nasahara, K.N., H. Muraoka, S. Nagai, and H. Mikami, 2008. Vertical integration of leaf area index in a Japanese deciduous broad-leaved forest, *Agricultural and Forest Meteorology*, *148*:1136-1146.

Nakai, Y., K. Kitamura, S. Suzuki, and S. Abe, 2003. Year-long carbon dioxide exchange above a broadleaf deciduous forest in Sapporo, Northern Japan, *Tellus*, *55B*:305-312.

Nishida, K., 2007. Phenological Eyes Network (PEN): a validation network for remote sensing of the terrestrial ecosystems. *AsiaFlux Newsletter*, *21*:9-13.

Ohtsuka, T., T. Akiyama, Y. Hashimoto, M. Inatomi, T. Sakai, S. Jia, W. Mo, S. Tsuda, and H. Koizumi, 2005. Biometric based estimates of net primary production (NPP) in a cool-temperate deciduous forest stand beneath a flux tower, *Agricultural and Forest Meteorology*, *143*:27-38.

Rouse, J.W., Hass, R.H., Schell, J.A., & Deering, D.W. (1973). Monitoring vegetation systems in the great plains with ERTS. *Third NASA ERTS Symposium*, *1*, 309-317.

Saigusa, N., S. Yamamoto, S. Murayama, and H. Kondo, 2005. Inter-annual variability of carbon budget components in an AsiaFlux forest site estimated by long-term flux measurements, *Agricultural and Forest Meteorology*, *137*: 4-16.

Saigusa, N., S. Yamamoto, S. Murayama, H. Kondo and N. Nishimura, N. 2002. Gross primary production and net ecosystem exchange of a cool-temperate deciduous forest estimated by the eddy covariance method, *Agricultural and Forest Meteorology*. *112*,:203-215.

Sands, P.J., and J.J. Landbergs, 2002. Parameterisation of 3-PG for plantation grown *Eucalyptus globules*. *Forest Ecology and Management*, *163*:273-292.

van Leeuwen, W.J.D., A.R. Huete, and T.W. Laing, 1999. MODIS vegetation index compositing approach: a prototype with AVHRR data, *Remote Sensing of Environment*, *69*:264-280.

Waring, R.H., J.J. Landsberg, and M. Williams, (1998). Net primary production of forests: a constant fraction of gross primary production, *Tree Physiology*, *18*:129-134.

Yamamoto, S. 2002. Aim of the CO_2 flux measurements network in different forest ecosystems in East Asia, *AsiaFlux Newsletter*, *1*:2-3.